

Main Controlling Factors of Regional High Geothermal Anomaly

Xiaoping Mao¹ and Kewen Li^{1,2}

¹China University of Geosciences (Beijing), 100083, China

²Stanford University, USA

likewen@cugb.edu.cn

Keywords: geothermal sweet spot, heat conductivity, tectonic movement, magma sac, mirror reflection

ABSTRACT

Finding the anomaly of high temperature is the key to the geothermal exploration. In this paper, the various factors that influence the temperature are analyzed. Taking the distribution of geothermal field in Cangxian uplift as case study example, forward modeling is conducted. It is found that the lateral heterogeneity of materials caused by tectonic movement is one of the main controlling factors of the regional geothermal field. Based on this observation, a "sweet spot model" for causing high abnormal temperature (geothermal anomaly) is proposed. It is pointed out that any anomalous heat source in the long history of geological evolution may not be sufficient to support the local or partial abnormal high temperature. The magmatic activity, radioactive heat generation and fault on the rock temperature may not be the only controlling factors. The temperature in the paleo-uplift area is characteristic of "mirrored reflection" in vertical direction in some cases.

1. INTRODUCTION

The development and utilization of geothermal energy, as a clean energy source, has been put forward for many years, which is of great importance to alleviating China's air pollution problem. At present, geothermal exploration and development have been conducted on a large scale in some countries (Tester et al., 2007; Erkan et al., 2007). And yet, there is still no extensively utilization in China. The reason is mainly because the cost of geothermal exploration and development is excessively high, and no geothermal field with great economic value has not been found, i.e., "geothermal sweet spot" area with shallow depth and high temperature. Therefore, it is of great significance to predict the favorable zone of geothermal exploration.

Geothermal resources, like other unconventional resources, belong to distributed resources. The sweet spot here refers as to the favorable zone with higher temperature and the lowest development cost under the same conditions. According to the present geothermal field cases, geothermal sweet spots do exist, such as the Well Yang-8 in Tibet and the Ganzi region of Sichuan Province, etc. However, the location of the geothermal field with industrial value is relatively remote, both in the far western and southwestern mountainous areas. It is necessary to find geothermal fields close to the developed areas for significance of practicality.

Many scholars have done a lot of studies on the causes of abnormal high temperature (Chapman and Rybach, 1985; Lee, 1970; Cermak and Rybach, 1989; Tao, 2000). At present, it is generally believed that the main factors of geothermal anomaly are fault zone, radioactive heat generation (radioactivity thermogenesis) and mantle activity. Gao et al. (2009) summed up the causes of abnormal geothermal based on practical experience, i.e., which is attributed to the heat convection with material exchange. The deep heat flow cycle in the old stratum (layer) leads to the thermal anomaly in the uplift zone.

Rock radioactivity is believed to have an impact on the geothermal activity, in which the major radioactive elements uranium, thorium and potassium, accounts for 5 – 6 times as much in the crust as in the mantle and core. According to Qiu (2002), the heat generated by radioactive thermogenesis of the rocks can account for about 25%~45% of the surface heat flow in the basin. In the crust, the radioactivity of sedimentary basin is more abundant than that of the crust. Dark mudstone is the main source rock of oil and gas in the basin. The geothermal gradient in almost all sedimentary basins is much lower than that in the marginal uplift zone of the basin. For example, in the Tarim Basin, the maximum thickness of the deposit is in the Manchar depression with a geothermal gradient of less than 20°C/km. In the center of Sichuan Basin, the geothermal gradient is even lower, as low as 16°C/km, which is much lower than average geothermal gradient of 30°C/km in mainland China. Therefore, it is impossible to confirm that the heat generated by radioactive enrichment of dark mudstone in the center of the basin is sufficient enough to change the thermal structure of the basin. As it can be seen from Figure 1, the largest number of sedimentary basins in China, except Songliao basin, the rest such as the Tarim Basin, the Junggar Basin, the Sichuan Basin and the Ordos Basin, have much lower temperature than those of the national average. In addition, another condition for enrichment of radioactive elements is magmatic intrusion. Due to the oxygen-friendly and polyvalent nature of radioactive element uranium, uranium is less precipitated in the process of intrusion, but eventually due to magmatic differentiation, it is only enriched in the contact zone between granite and surrounding rock, and its radioactivity is still insufficient to change the entire geothermal field. Few of the geothermal field found at present shows the decisive effect of radioactive heat generation on geothermal fields. It can only act as the background geothermal field and superposition the geothermal flow in the earth's crust.

Some believe that the material heterogeneity on a large scale, such as crust and mantle thickness, is the main factor. Han and Jin (2002) conducted a study and analyzed the geothermal resources and thermal structure of Northeast China from the statistical point of view. Based on the statistical analysis, it is considered that the thermal structure of the crust and upper mantle in this area has caused the change of heat flux distribution. There is a positive correlation between the Moho fluctuation and the distribution of the geothermal field, that is,

the higher the uplift, the higher the temperature. In fact, for the large area of the whole country (China), there is a positive correlation between the fluctuation of the Moho surface and the distribution of the geothermal field. This observation is inconsistent with the distribution of the actual geothermal field. Figure 1 shows the map of the geothermal distribution of 5.5km depth in China. The crust in Tibet is thicker and it is supposed to have low temperature, but there are still anomalies of high geothermal temperature. Hence, there is no direct relationship between geothermal distribution and crustal thickness on large regional scale.

The fault has great influence on the local geothermal field. Tao and Liu (2000) studied the forming factors of hot springs in the Tanlu fault zone and its adjacent area. It is found that the development of hot springs in the Tanlu fault zone and its adjacent area depends on the existence of geological heat source, regional structure, fault and groundwater circulation, thermal conductivity of basement and caprocks, etc. If the fault is used as a clue to search for geothermal anomaly, there may be problems. As a matter of fact, if we observed at the large area in Figure 1, the geothermal temperature of North China Plain is relatively high, but in the east of the Tanlu fault zone, there's no obvious anomaly of geothermal height. The geothermal field of Cangxian developed at present is 260 km northwest of the fault. So, it can be considered that the geothermal anomaly has little relationship with the distribution of fault zone.

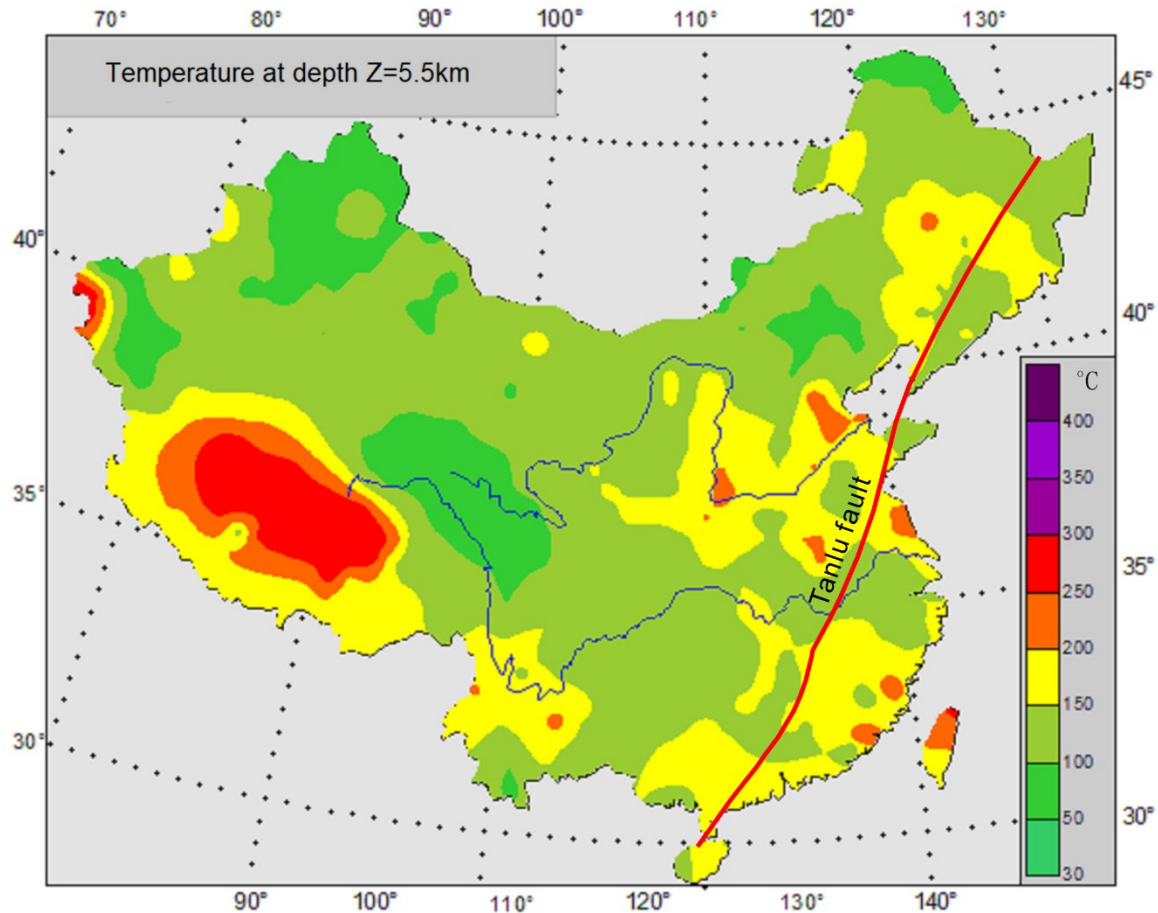


Figure 1: Geothermal distribution in China at Depth $Z=5.5\text{km}$ (Wang, et al., 2012)

Many believe that magmatic intrusion is the main controlling factor of geothermal field (Berktold, 1983; Oskooi et al., 2005; Urzua et al., 2002). Bai et al. (2006) investigated the unique crustal structure and high heat background of the Qinghai-Tibet plateau, and concluded that the southern Himalayan block belongs to the “hot crust and cold mantle” type. The Lhasa-Gangdis terrain belongs to the “hot crust and hot mantle type”. There is low velocity and high conductivity layer in the middle crust of this area, which may be part of the molten magmatic sac, forming a grand scale tropical geothermal zone.

Many scholars have done statistical research on the influence of basement fluctuation and overburden thickness on the geothermal field, which is considered to have a great influence on the temperature field (Ma et al., 1983; Yan and Lu, 2000). Chen and Deng (1988) remarked that underground heat flow always shifted to the part with high thermal conductivity and low thermal resistance in the conduction process, and it was easy to form the thermal anomaly, and suggested that the uplift belt zone had high temperature anomaly. There is a positive correlation between the temperature and the basement fluctuation. Gong et al. (2003) studied the distribution characteristics of terrestrial heat flux in Jiyang depression. They reported that the transverse variation of the heat flux is positively related to the base fluctuation, but it is attributed to the effect of “thermal refraction” effect (Wang et al., 2002). Thus, the heat accumulated to the uplift of

the depression. The distribution of the relative high heat flux and the Cenozoic volcanic rocks are roughly compared and analyzed. The results show that the heat flow is closely related to the magmatic activity of the Cenozoic.

To sum up, there are many factors influencing the formation of a geothermal field. How to locate the most crucial factors out of these and put forward a model of predicting favorable geothermal zone is the focus of this paper.

2. FAST DECLINE OF ABNORMAL GEOTHERMAL TEMPERATURE

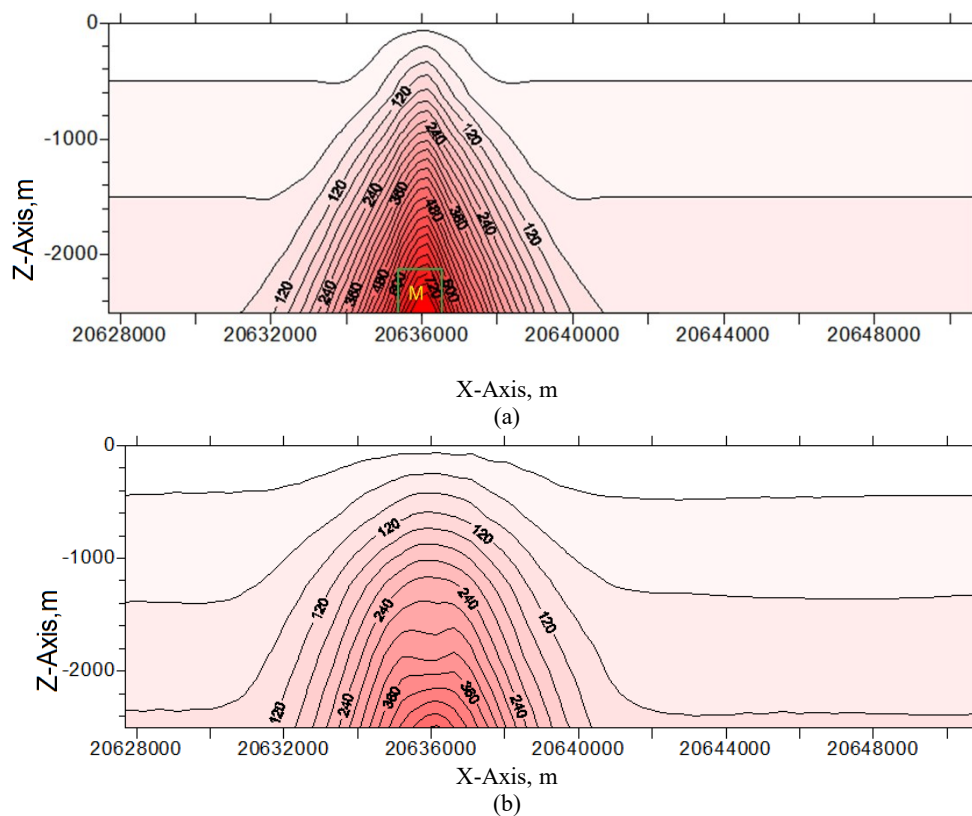
In order to show the cooling velocity of geothermal anomaly, we conducted a 2-D numerical simulation of heat conduction using finite difference method. Assuming that the formation is homogeneous, the magma invades at 800 °C (thermal conductivity $k=1.4 \text{ W/m}\cdot\text{°C}$), with an amplitude of $1 \times 1 \text{ km}^2$ (green line in Figure 2a). The model was discretized to form a rectangular grid of 71×76 and the length and height was $23 \times 2.5 \text{ km}^2$, and the average temperature of the earth surface was assumed to be 15°C and the geothermal gradient was 30°C/km . The thermal conductivity of the skeleton is $2.2 \text{ W/(m}\cdot\text{°C)}$. The modeling was conducted using the two-dimensional thermal conductance equation as follows:

$$\frac{\partial}{\partial x} \left(k_x \frac{\partial T}{\partial x} \right) + \frac{\partial}{\partial z} \left(k_z \frac{\partial T}{\partial z} \right) + Q = \rho c \frac{\partial T}{\partial t} \quad (x, z) \in D \quad (1)$$

Where T is paleogeotemperature; t is time (s); k is underground rock heat conductivity ($\text{W/m}\cdot\text{°C}$); ρ is stratum density (kg/m^3); c is the specific heat of underground rock ($\text{J/kg}\cdot\text{°C}$); Q is abnormal geothermal source such as rock mass intrusion (W/m^3); D is the space range of the modeling.

Figure 2 is the sectional temperature field distribution at different period. Figure 2a shows the initial temperature section under the initial condition of ($t=0\text{Ma}$) when rock mass intrudes. The highest temperature is 800°C . After simulated calculation, the temperature difference will fall to 500°C after 0.02Ma ($1\text{Ma}=1000 \text{ 000 years}$), higher than 495°C of the background field as shown in Figure 2b. It will decrease to 240°C after 0.06Ma , higher than 135°C of the background field (See Figure 2c). It will descend to 180°C , higher than 75°C of the background field after 0.1 Ma , as shown in Figure 2d. After 0.3Ma , the abnormal geothermal temperature will disappear (see Figure 2f).

Thus, it can be seen the cooling process of geothermal anomaly is fast and equilibrium temperature can be reached within 0.1 to 0.3Ma .



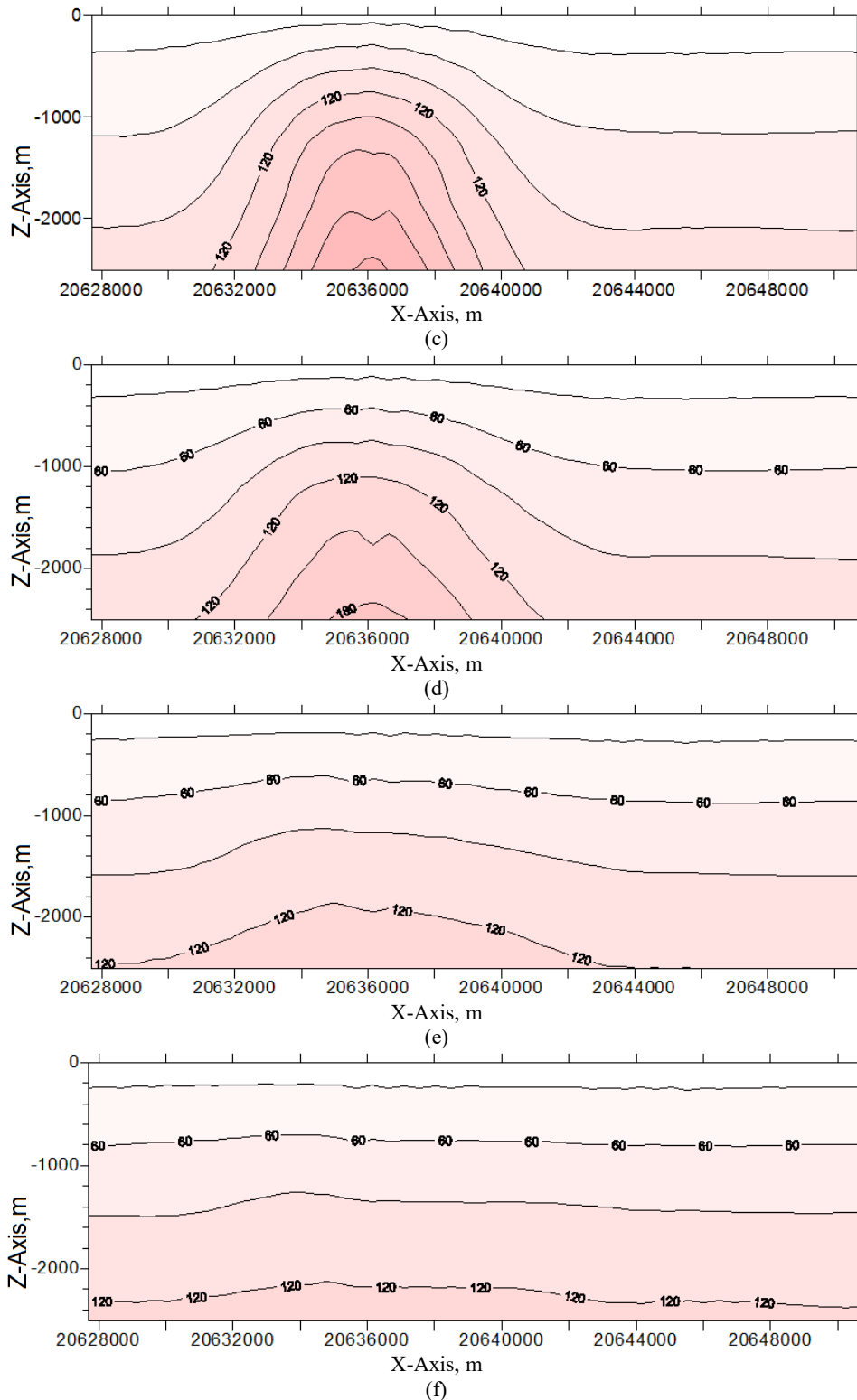


Figure 2: Temperature distribution profile at different times after the intrusion of magma (a) 0Ma (b) 0.02Ma (c) 0.06Ma (d) 0.1Ma (e) 0.2Ma (f) 0.3Ma

Previous scholars had similar simulation conclusions. Studies of Lovering (1959), Rikitake (1959) and Mundry (1968) showed that the cooling rate of the intrusive body is related to its volume and the cooling rate of magma is faster than that geological history. as shown in Table 1. For example, in the case of Dyke of 200m thickness, it only takes 6,500 years to reduce to 10% of the original temperature.

Table 1: Required time for magmatic intrusion object to cool to 10% of the original temperature (year) (According to Gretener, 1988)

Magmatic rock body	Lovering(1959)	Rikitake(1959)	Mundry(1968)
Plutonic mass R= 1km	26 000	25 000	30 000
R=2km	105 000	100 000	105 000
Volcanic neck cylindrical R=1km			100 000
(Stock) R=2km			500 000
Dyke (clintheriform) H=10m	16		15
Dyke (Sill) H=100m	1 600		2 000
Dyke H=200m	6 500		6 000

Note: R is the radius of the magmatic rock body and H represents its thickness.

Tian et al. (2005) conducted magmatic activity thermal simulation and investigated its effect on source rock thermal evolution. They concluded that the cooling time of the intrusive body increases with the depth and increases with the thickness of the intrusions. Table 2 listed the intrusive temperature of 800°C, different intrusive depths, different thickness, required time for temperature difference lower than 5°C between the place of the intrusive body and the surrounding rock. It can be seen from simulation results in Table 2 that the time required for cooling of the intrusive body increases as the depth goes further and the thickness is enhanced. However, the cooling time of most of intrusive bodies is within 1Ma.

Table 2: Estimation of time (0.01Ma) required for sill-like intrusive body to cool (Tian, et al., 2005)

Depth/m	Thickness, m				
	50	100	200	300	400
1000	4.5	7	11.5	15	18
2000	8.5	15	27	37	45
3000	11.5	25	45	62	77
4000	13.0	32	62	87	110

Figure 3 shows changes in superheat temperature of surrounding rocks with changes in time at different depths after magmatic intrusion in heat simulation. It can be noted from the chart that the evolution history of superheat temperature of surrounding rocks with the same distance from the intrusive body above and below is basically the same. No matter how far it is from the intrusive body, the surrounding rock's temperature quickly rises and will slowly go down after the highest temperature. The rising temperature of the surrounding rock is no more than 200°C. It reaches a peak after 500 to 1,000 years, 100-200°C. It will fall to the normal temperature of 60°C after 0.01Ma, 20°C after 0.2Ma and border on zero after 1Ma, that is, balanced temperature.

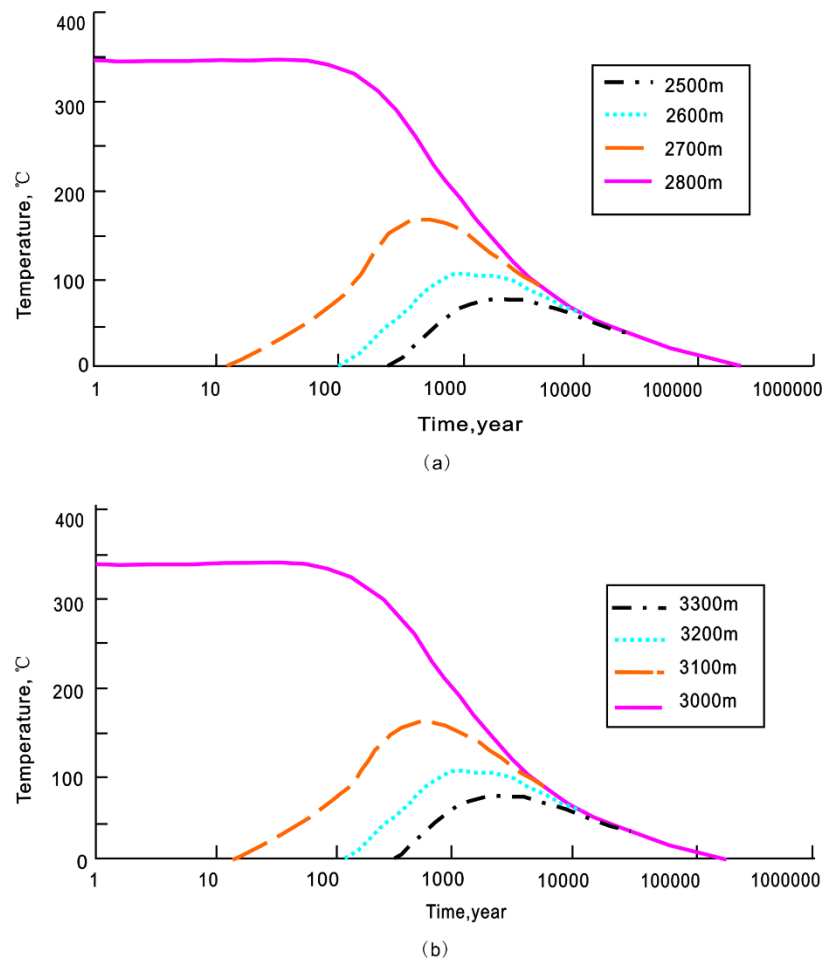


Figure 3: Changes of surrounding rock superheat temperature with time change at different depths (Tian, et al., 2005)
(a) Surrounding rock above the intrusive body; (b) Surrounding rock below the intrusive body
 (Note: the intrusion depth is 2800~3000m; the intrusion temperature is 800°C; the thickness is 200m)

Zhang et al. (2013) investigated the cognition of “magmatic thermal field” in geothermal field and its significance and proposed that once magma cool down and the temperature difference between rock body temperature and surrounding rock is zero.

The above research and simulation results indicate that the geothermal anomaly produced by magmatic activity will quickly cool down with heat conductance and reach a dynamic equilibrium. Based on the result, it is debatable to explain the origin of the high temperature of Well Yang-8 by magmatic activity and magma heating directly for heat fields unless it is proved that high-temperature magma intruded within one to 0.1Ma. As a matter of fact, Wu et al. (2005) conducted a thermochronological analysis of the heat evolution history of granite in Nyenchen Tanglha and held that early stage magma emplacement incident happened at 65.0~55.0Ma; large-scale magma emplacement and crystallization incidents took place at about 11km depth during 18.3~11.1Ma. At 11.1Ma (=11.1 million years), the magma intrusion ended and it still had sufficient time to cool down.

In summary, unless the rock mass is still intruding and moving within recent 200,000 to 500,000 (note: the quaternary starts from 1.64Ma) and still disturbs temperature field, influences of most rock mass intrusions over today’s geothermal field may be ignored. Hence, the geothermal exploration model of supplying heat for geothermal field by relying on “magma pocket” may need to be further considered.

3. RELATIONSHIP BETWEEN THE BASEMENT TECTONIC FLUCTUATION AND THE GEOTHERMAL FIELD

According to the foregoing, we believe that one of the main controlling factors determining the distribution of the regional temperature field is the lateral heterogeneity near the surface. Both theoretical simulation and actual geothermal exploration indicate that the lateral heterogeneity such as basement tectonic fluctuation affects the geothermal field.

A positive correlation between the shape of the basement fluctuation and the geothermal gradient curve has been recognized for a long time, and the thermal conductivity of the strata is positively correlated with the age of the formations. The older the age, the higher the thermal conductivity. The thermal conductivity of igneous rocks is higher than those of the sedimentary rocks, and the fluctuation of the basement or magmatic intrusions lead to the differences in thermal conductivity. Xiong and Zhang (1998) studied influences of basement

fluctuation on geothermal field through 2D heat conduction forward modeling. As shown below (Figure 4), two kinds of media were set up: the basement and the surrounding rock. They are below ABCD is the basement and above is the surrounding rock. A part of the basement is protruded to Line CD in the paleouplift, and the lithology of AB is the same as that under the depth of AB, which is referred to as the homogeneous depth of lithology. The modeling results show that there are different temperatures in different parts. At the top CD of the basement uplift, the temperature is 10-25°C higher than that at the E point of the background temperature. The lithologic homogenization depth is basically the same, as shown in the diagram of point A, B and H; under the homogeneous depth of lithology A and B, there will be negative abnormal temperature, that is, the temperature of G spot in the uplift area is still lower than the background temperature of surrounding rock, for example, in point F, "Mirror reflection" appears in the isothermal of the section. The temperature difference is related to the thermal conductivity, which indicates that there is a positive correlation between the geothermal gradient and basement fluctuation.

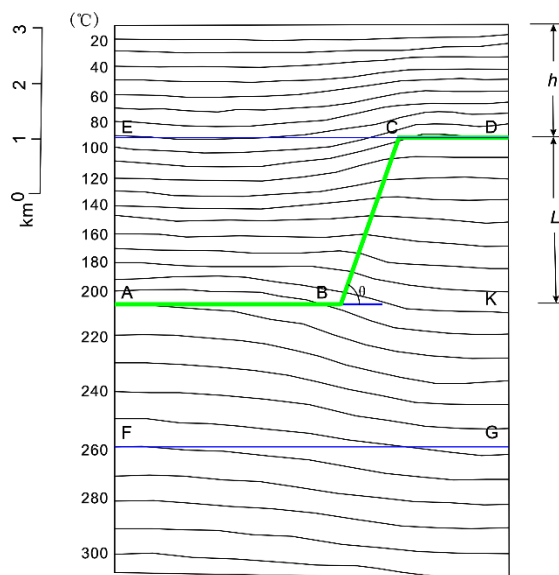


Figure 4: Finite element method ground temperature calculation model and calculation results (Xiong and Zhang, 1988)

As shown explicitly, through the forward modeling of the temperature field, it is clear that the geothermal anomaly is related to the basement fluctuation. The basement fluctuation is only a representation, and the essence is the heterogeneity of the formation physical properties, i.e. the difference of the thermal conductivity due to transverse or horizontal material inhomogeneity. The high thermal conductivity basement on the right side has the function of fast heat transfer in relation to the surrounding rock on the left side, so the ground temperature is relatively high, and the difference always exists because of the transverse heterogeneity of lithology caused by the structure. The loss of the near-surface and the heating of the mantle is a dynamic equilibrium process, the heat cannot be accumulated. Abnormal cooling is fast, so macroscopically it is caused by the structure. In essence, it is the dynamic equilibrium process of the ground temperature caused by the lithologic difference.

Jiang and Xu (2013) also showed a similar phenomenon through forward modeling. In the high-conductivity uplift area, there is a high temperature anomaly above the homogeneous depth of lithology, and low temperature anomaly below it. This phenomenon can be explained by the existence of high conductor, which makes the deep part rapidly cooled and lower than the background field, while the shallow part of the rapid warming is higher than the dynamic equilibrium of the background field. This may imply that shallow geothermal field needs to be found in the uplift area and deep geothermal needs to be found in the basin area.

Zhou et al. (1989) studied the geothermal field in Xiong, and realized that the high geothermal field may be related to bedrock uplift. Figure 5 shows that the direction of the profile is East-West, and the caprocks on the section are similar in thickness. In this case the basement fluctuation is the decisive factor. In Xiong well-9 of Niutuozen uplift around Xiong County, the bedrock is relatively shallow, the geothermal gradient reaches the highest 66 °C/km, and the Rong-1 well of Rongcheng uplift reaches 58 °C/km. Well Jia-1 in Baxian sag is 46 °C/km, while in the middle, the basement is deep and the geothermal gradient is low, which is consistent with the previous discussion.

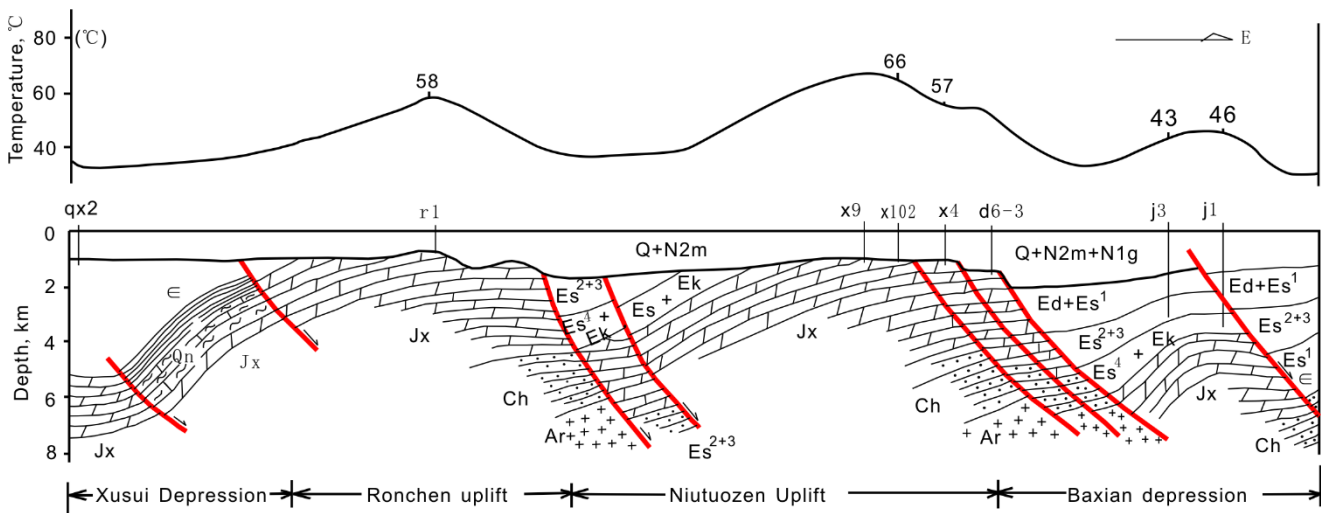


Figure 5: Niutuozen thermal field and thermal geological section chart (Zhou et al., 1989)

In many of the geothermal fields, temperatures in vertical direction are of mirror reflection, such as Yang Yi geothermal well ZK212, below 400 m temperature gradient dropped sharply to 24°C/km (Liu, 2014). The geothermal gradient of the borehole ZK302, ZK303 below 160m is close to 0°C/km in Well Yang-8 (Hu, 1992). In Schultz the measured temperature distribution in the region of France, in the depth of below 1.4 km the geothermal gradient is very small (Baria and Baumgärtner, 1994). In Ganzi, a drilling temperature profile, at 150m depth temperature reached 90 °C, and then deep drilling to the depth of 600m, the temperature is almost not changed (Wu, 2013); The geothermal temperature of well ZK1 in Xinzhou geothermal field of Yangjiang quickly reached 75-80°C within the depth of 80m-160m, the temperature increases slowly down to 700 m, only to 95 °C, and to 1000m to 106 °C (Lan and Gan, 2016).

4. THE INFLUENCE OF THE CAPROCKS ON THE TEMPERATURE FIELD

Similar to the caprocks of oil and gas, it plays a role in capping resources and is the necessary condition for geothermal anomaly but not the controlling factor. Thermal caprocks refers to geothermal overburden, whose thermal conductivity is lower than that of the surrounding rock, which can be called geothermal high resistance layer, far lower than high conductivity layer, and can slow down heat loss. It is concluded through simulation study that the suitable thermal caprocks thickness should be 100 to 500m. If it is too thin, the heat cannot be kept. Jiang et al. (2013) showed through geothermal forward modeling of Baoding-Qikou section that there is a low temperature anomaly in these area because of the outcropping of Archaean in Western Baoding because there is no Cenozoic caprock. They also showed that in Cangxian uplift there are high temperature anomalies in shallow area due to the existence of a specific cover and high conductivity layer of the basement.

4.1 Influence of caprocks thickness on temperature

It has become a consensus that there must exist caprocks for geothermal reservoirs to reach a certain temperature, but how much thermal resistance and thickness of caprocks can meet this requirement need a quantitative analysis. For this, the above-mentioned 2D heat conduction simulation is used here again.

4.1.1 Basement with medium thermal conductivity

In order to investigate the influence of caprock thickness on the temperature field, a wedge model was designed with two sets of strata: geothermal reservoir (k_2) and heat caprocks (k_1). In order to avoid the "thermal refraction" effect, the length of the model was set to be 20 km. The results of the analysis are shown in Table 3. The thermal conductivity k_2 of geothermal reservoir is 4.43W/(m·°C), the surface boundary condition (surface temperature) is fixed at the annual average temperature of 15 °C; the temperature at the bottom of the model is not fixed, a basement heat flux 65.31mW/m² is set constant, and the initial condition of the model is set to meet the initial geothermal gradient: 30°C/km. The temperature field profile of the model with $k_1=0.6W/(m·°C)$ was calculated and the results are listed in Figure 6. The depth data corresponding to 50°C、60 °C、70 °C were identified (Table 3). The implication is that when the thermal conductivity k_1 of the caprocks is 0.6W/m·°C and its thickness is 372 m, the bottom reservoir temperature can reach 50 °C after the temperature is in equilibrium. If the geothermal reservoirs at the bottom of the caprocks reaches 70 °C, the thickness of the caprocks needs to be at least 593.1 m, that is, the geothermal reservoir at 593.1 m can reach 70 °C. In the same way, the thickness required for specific temperatures at different thermal conductivity of geothermal caprocks ranging from 0.2 to 10 were obtained. These data are used to explain the influence of the thickness of thermal caprocks on temperature.

It can be seen from Table 3 that when the thermal conductivity of the caprocks is lower ($k_1=0.2 W/(m·°C)$), the temperature of 50 °C can be reached at the shallow depth of the caprocks ($H=135.5m$). When the thermal conductivity of the geothermal caprocks is high, it is necessary to reach a very deep place ($H=1130.7m$) to reach 50 °C.

The two curves of the upper part of Figure 6 are the temperature distribution curves of 500m and 1000m depth, respectively. It can be seen from the diagram that the temperature difference between the left side of the section without caprocks and the condition of right side with caprocks is up to 60°C (H=1000m). It can be seen that certain thickness of caprocks is a necessary condition.

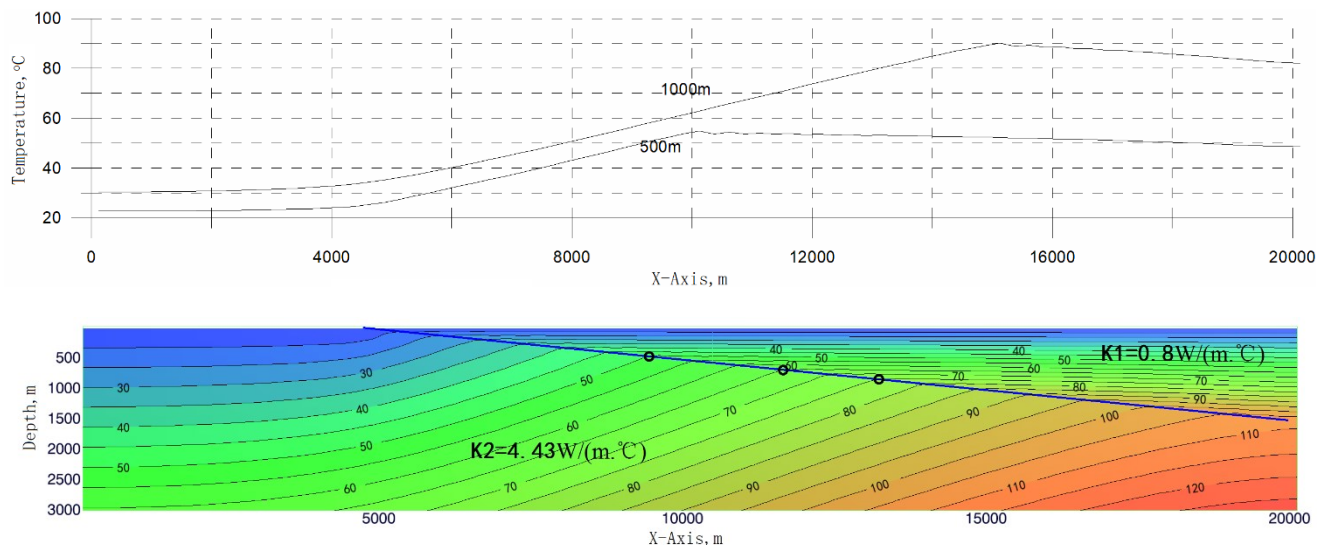


Figure 6: Geothermal field of the wedge-shaped profile model ($k_1= 0.8 \text{ W}/(\text{m}\cdot^\circ\text{C})$, 0.4Ma)

Table 3 Caprocks thickness and reservoir temperature correlation
(with medium basement thermal conductivity)

Thermal conductivity of caprocks k_1 $\text{W}/(\text{m}\cdot^\circ\text{C})$	Thickness (m) to 50°C	Thickness (m) to 60°C	Thickness (m) to 70°C
0.2	135.5	177.3	225.0
0.4	254.5	329.7	406.1
0.6	372.0	480.0	593.1
0.8	482.1	620.2	754.9
1.0	591.3	757.7	927.7
1.2	701.0	902.0	1118.0
1.4	807.0	1038.5	1291.9
1.6	917.3	1182.5	1515.0
1.8	1022.6	1334.2	-
2.0	1130.7	1502.0	-

(Note: $k_2=4.42 \text{ W}/(\text{m}\cdot^\circ\text{C})$; basement heat flux $65.31\text{mW}/\text{m}^2$)

4.1.2 Basement with low thermal conductivity

Table 4 is similar to Table 3, except that the basement conductivity is $3.0 \text{ W}/(\text{m}\cdot^\circ\text{C})$, while other parameters are unchanged. Also take $k_1=0.6 \text{ W}/(\text{m}\cdot^\circ\text{C})$ as an example, to ensure temperature of the thermal reservoir to reach $50, 60,$ and 70°C , the caprocks must be thicker than 368.3m and 468.6m respectively.

Table 4: Caprocks thickness and reservoir temperature correlation
(with low basement thermal conductivity)

Thermal conductivity of caprocks k_1 $\text{W}/(\text{m}\cdot^\circ\text{C})$	Thickness (m) to 50°C	Thickness (m) to 60°C	Thickness (m) to 70°C
0.2	133.1	173.6	220.9
0.4	251.7	323.5	394.6
0.6	368.3	386.2	468.6
0.8	473.6	603.8	734.0
1.0	581.0	740.9	903.2
1.2	700.0	898.0	1105.0
1.4	793.2	1017.5	1248.1
1.6	899.1	1154.1	1431.3
1.8	1004.6	1295.3	-
2.0	1112.7	1439.6	-

(Note: $k_2=3.0 \text{ W/(m}\cdot\text{°C)}$; basement heat flux 65.31mW/m^2)

4.1.3 Basement with high thermal conductivity

Some basement may have higher thermal conductivity. As shown in Table 5, when $k_2=6.0 \text{ W/(m}\cdot\text{°C)}$, $k_1=0.6 \text{ W/(m}\cdot\text{°C)}$, while other parameters are kept constant, to ensure temperature of the thermal reservoir to reach 50, 60, and 70 °C, the caprocks must be thicker than 377.6m and 601.6m respectively.

Table 5: Caprocks thickness and reservoir temperature correlation
(with high basement thermal conductivity)

Thermal conductivity of caprocks k_1 $\text{W/(m}\cdot\text{°C)}$	Thickness (m) to 50°C	Thickness (m) to 60°C	Thickness (m) to 70°C
0.2	136.7	180.4	230.5
0.4	258.1	337.1	421.3
0.6	377.6	488.5	601.6
0.8	491.7	633.5	778.8
1.0	603.6	776.7	964.8
1.2	717.7	922.0	1143.5

(Note: $k_2=6.0 \text{ W/(m}\cdot\text{°C)}$; basement heat flux 65.31mW/m^2)

Figure 7 shows the temperature field result of the wedge-shaped model after 1.2Ma when k_2 is 6.0 $\text{W/(m}\cdot\text{°C)}$ and k_1 is 1.2 $\text{W/(m}\cdot\text{°C)}$.

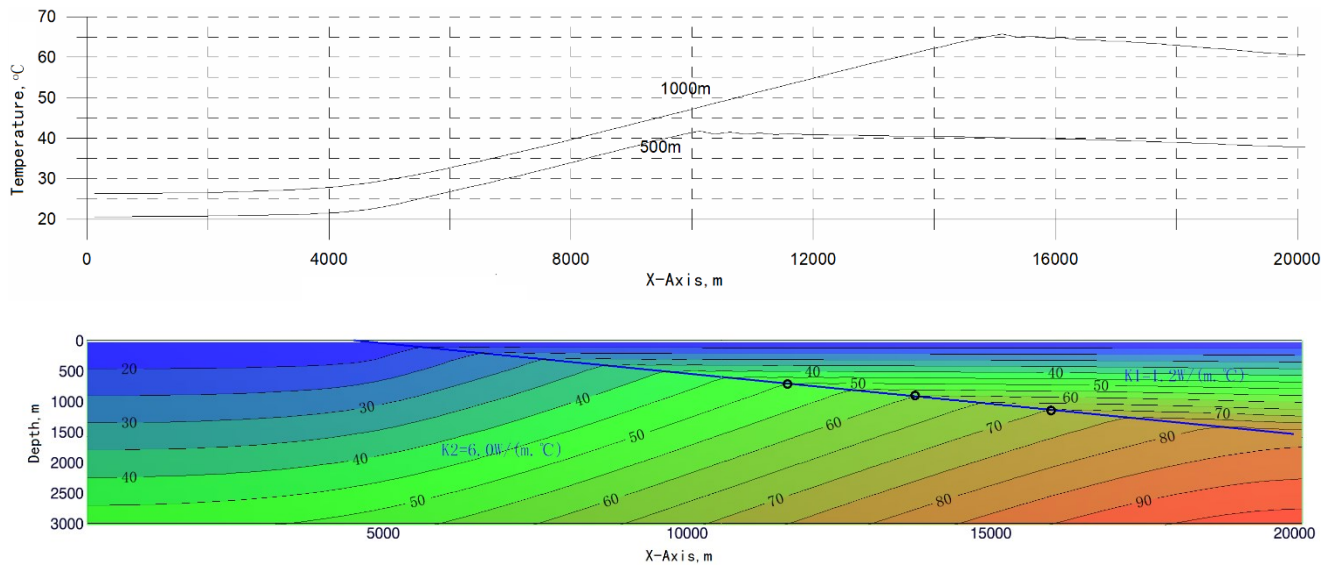


Figure 7: Temperature field of the wedge-shaped profile model ($k_1= 0.8 \text{ W/(m}\cdot\text{°C)}$, 1.2Ma)

From the three-different thermal conductivity of the basement, no matter whether the thermal conductivity of the basement is, low or high, the influence on the thickness of result is not very great. The thickness of the heat caprocks required to reach a specific temperature is closely related to the thermal conductivity of the caprocks itself.

4.2 The effect of the caprocks on the temperature field in some actual cases

Figure 8 shows two cross sections across Cangxian uplift and Chengning uplift in Beijing-Tianjin-Hebei area. The Proterozoic strata of Cangxian and Chengning uplift are buried shallowly, and they are a set of high conductance layers, which directly cover the Cenozoic strata. The thermal caprock is a typical paleouplift with a certain extent. The second uplift is distributed from north east to south west towards the northeast of Tianjin with low temperature. The I-I' caprock in the section is thin and the geothermal gradient is middle and high in the uplift of Cangxian. The section I-II' caprocks is thick enough (500-700m) and the geothermal gradient is the highest. The southwest overburden is thicker, which belongs to middle and high, but buried deep. The fluctuation of basement strata has obvious positive correlation with the lateral variation of ground temperature, that is to say, the depression zone is a low temperature zone. The uplift zone is a high temperature anomaly zone. But if there is no certain thickness of cap or high resistivity layer, this rule will fail. For example, there is a large area of high conductivity strata and Proterozoic strata and granite outcrop in northwest Beijing. However, there is no abnormal high temperature display as shown in Figure 8 because it does not have a thermal cap, which fully illustrates the necessity of the thermal cap.

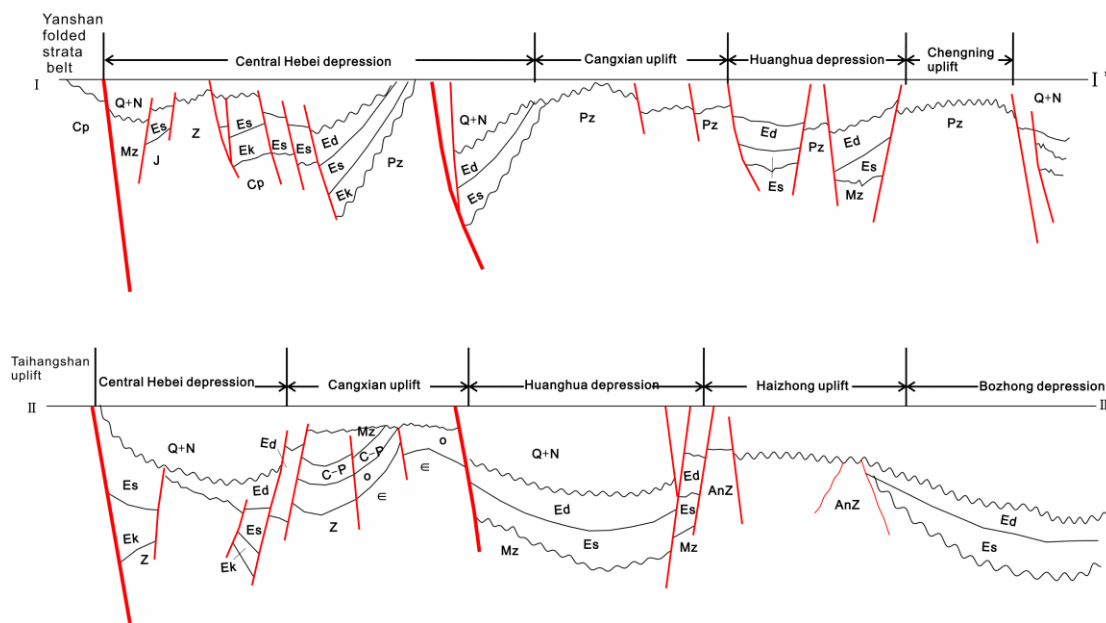


Figure 8: Geological profile across Cangxian-chengning uplift in Beijing, Tianjin and Hebei region (Yan and Yu, 2000)

Chen Moxiang (1990) also reported the influence of the Cenozoic caprocks on the temperature in the North China Plain. The depth of burial was 1000 meters in the geological section through the Jizhong Depression Cangxian uplift and Huanghua Depression. From the geothermal gradient of 2000 meters, it can be seen that Cangxian uplift has the highest geothermal temperature from the hot cap, while the southwest of Baoding sag has high conductance, which reduces the geothermal gradient due to the absence of overburden.

5. GEOTHERMAL SWEET SPOT MODEL

Geothermal sweet spots are the most favorable geothermal area with a higher temperature background field of the region. Because of the existence of high thermal conductivity in this area, the geothermal temperature is higher than that of surrounding rock under certain cover conditions, that is, the local geothermal temperature in the crust is abnormally high. The following diagram (Figure 9) is taken as an example to illustrate the main conditions for the formation of geothermal sweet spot. Due to various geological tectonic activities, the high heat conduction layer A extends to the shallow surrounding rock B and C and extends to a certain extent. A "positive terrain" basement is formed, with a high thermal resistance or low heat conduction layer D above the surrounding rock, that is, the geothermal sweet spot pattern map. Due to this lateral difference in lithology, the high thermal conductivity layer A serves as a "fast heat transfer channel" because of the difference in the horizontal direction of the physical property relative to the surrounding rock, and make the temperature field a geothermal skylight above R2. The temperature at the top of the high thermal conductivity layer (A1) will be higher than that of the surrounding rock. In other surrounding rock areas, such as R1 and R3, the heat transfer speed of the deep heat source is slower when it meets the sedimentary formation (B, C) or low heat conduction layer, compared with R2, the temperature is lower at the same depth. The skylight makes the heat flow of the mantle a fast heat transfer channel, which allows heat to quickly enter a shallow layer and quickly release the heat from the earth.

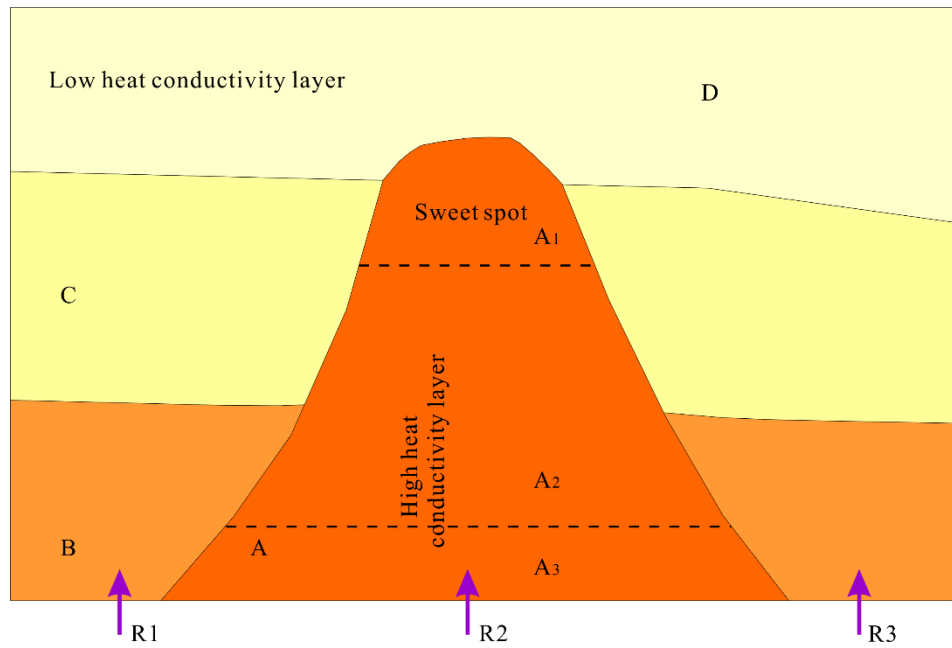


Figure 9: Geothermal sweet spot model section chart

There are 2 elements for geothermal sweet spot model: 1) higher heat conductivity layer is developed in the shallow location with a certain difference of depth, and the larger the difference, the better; 2) favorable heat caprocks with low heat transfer coefficient. The geothermal sweet spot model can be used to explain the main geothermal fields in China: Hot-Sea geothermal field in Tengchong, Yunnan and Tibet Well Yang-8 Geothermal Field.

At present, most researchers believe that Hot-Sea geothermal field in Yunnan Tengchong comes from the “abnormal heat source” magma sac because of active modern volcanos (Zhao and Ran, 2011; Jiang, et al., 2012; Guo, 2012). As a matter of fact, its volcanic activities are divided into four stages since 2Ma: 3.5-5.0Ma, 2.3-2.9Ma, 1.0-1.5Ma and 0.5-0.7Ma (Wang et al., 2015). The recent magmatic activity is 0.5Ma ago. According to previous analysis, the magma which has not erupted and stayed in the shallow layer forming magma chamber shall be as cool as the surrounding rock. The temperature field in the following section shown in Figure 10 can be easily explained by the sweet spot model, it meets two necessary conditions: high conductivity granite intruding body directly extends into the near-surface (heat conductivity $2.46\text{W/m}\cdot^{\circ}\text{C}$); the middle section is covered with 300-1000m of the Neogene thermal caprocks (Figure 10). High temperature anomaly exists under the caprocks. The heat is lost and there is no high temperature anomaly at the ends of section because the base rock on both sides of the section is exposed to the surface. In other words, this region does not need the concept of “magma sac” to explain causes for its high temperature anomaly.

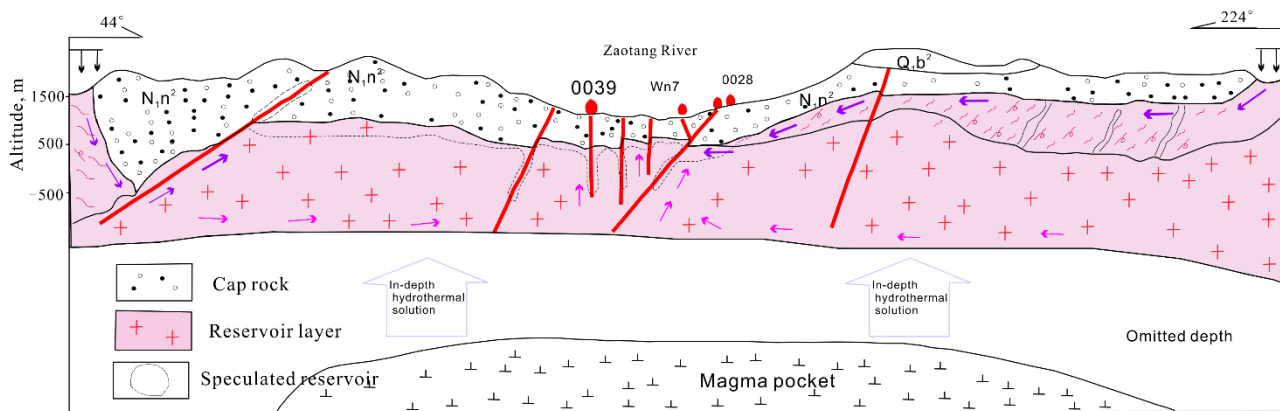


Figure 10: Concept model of Hot-Sea geothermal field in Tengchong (Guo, 2012)

In addition, the anomaly of high temperature in the Well Yang-8 geothermal field in Tibet, the most famous one in China, can also be explained by the viewpoint of geothermal sweet spot model put forward in this paper. For a long time, the cause of this geothermal field is believed to be the continuous heating of magmatic fluid in the deep part of the field (Yao and Zhang, 1986; Shen and Wang, 1984). As far as magmatic activity is concerned, Wu et al. (2001) studied the tectonic-thermal events occurring in the hinterland of the Qinghai-Tibet Plateau since the middle and late Mesozoic. The most recent two periods were the strong tectonic uplift events along the Gangdis

tectonic-magmatic belt at 25-15 Ma and the regional rift-uplift events in the middle of the Lhasa block since 8-6.5 Ma. The third phase is 15 million years old. Compared with the cooling time of the rock mass mentioned above, the magma has already entered a thermal equilibrium state after the intrusion. If explained by the geothermal sweet spot model, there are also two conditions, as shown in Fig. 11. The granite with high thermal conductivity (thermal conductivity $2.32 \text{ W} / \text{m} \cdot ^\circ\text{C}$) developed in shallow layer, and in the high temperature anomaly area, there is a loose accumulation of 300-800 m thick (thermal conductivity $< 0.6 \text{ W} / \text{m} \cdot ^\circ\text{C}$). However, the thermal conductivity of the two sides of the bedrock (gneiss) is close to that of the granite, which indicates that the caprock is a necessary condition.

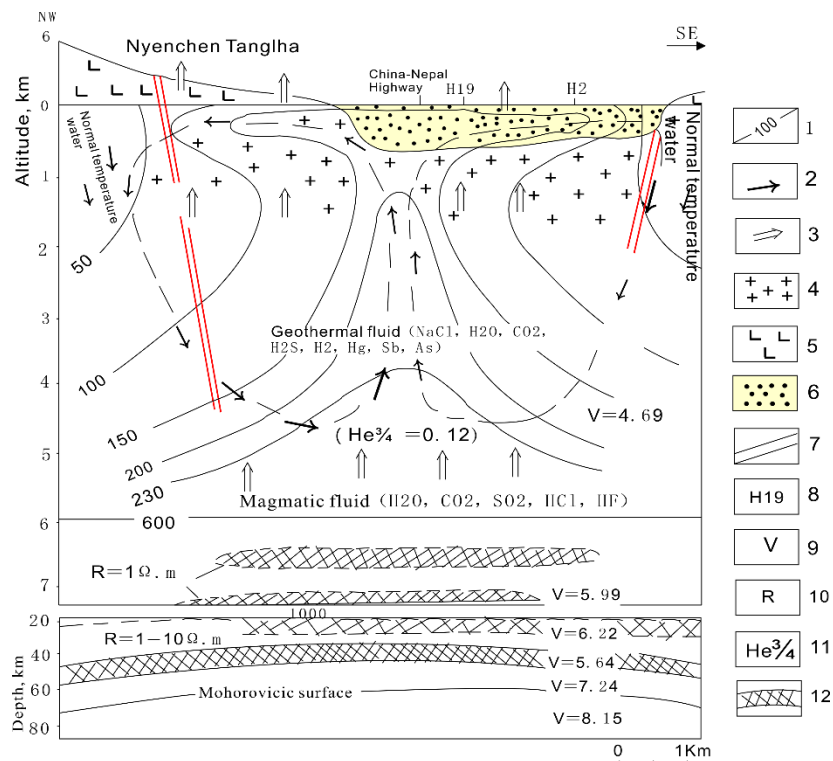


Figure 11: Sketch map of Tibet hydrothermal activities Well Yang-8 basin mechanism (Yao and Zhang, 1986)

1-isotherm; 2-geothermal fluid circulation line; 3-magmatic activity fluid direction; 4-granite Y6; 5-gneiss; 6-the quaternary system loose stack; 7-main fault; 8-main drilling position; 9-longitudinal wave velocity km/s; 10-magnetic earth current deep measurement (Ωm); 11-gas helium; 12-low velocity layer, low resistance object.

6. CONCLUSIONS

The following conclusions may be obtained through the forward modeling of the geothermal field and the comprehensive study of the actual data:

- (1). The heat dissipation time of magmatic intrusion and any high temperature anomaly body is relatively short, less than 0.1 to 0.2 Ma, compared with geological history. Hence, geothermal anomaly may not just rely on abnormal heat sources such as magmatic intrusion and radioactivity unless active quaternary rock mass still exists in the research zones.
- (2). The correlation between the distribution of the temperature field and the fluctuation of the basement is only a superficial phenomenon and its essence may be attributed to the heterogeneity of the shallow physical properties- heat conductivity. Such heterogeneity might be one of the main controlling factor of regional geothermal field. Relief of basement fluctuation and geothermal gradient shape has a positive correlation.
- (3). The caprocks with specific thickness is the necessary condition to form high geothermal anomaly. The lower the heat conduction coefficient of the caprocks, the easier it is to form high temperature anomaly in the shallow reservoir.

REFERENCES

- Bai, J., Mei, L., and Yang, M. L.: Geothermal resources and earth crust heat structure in Qinghai-Tibet Plateau J. Journal of Geomechanics, Sept., 12(3), (2006), 354-362.
- Baria, R, Baumgärtner, J, Gérard, A.: Status of the European hot dry rock geothermal programmer J. Geothermal Engineering, 19(1/2), (1994)33-48.
- Berktdold, A.: Electromagnetic studies in geothermal regions. Geophysical Surveys, 6(1-2), (1983), 173-200.

- Cermak, V and Rybach, L.: Vertical distribution of heat production in the continental Crust J. Tectonophysics, 159, (1989), 217-230.
- Chapman, D. S. and Rybach, L.: Heat flow anomalies and their interpretations J. J. Geodynamics, 4, (1985), 3-37.
- Chen, M. X. and Deng X.: Geothermal Gradient of Cenozoic Era in North China Plain and Its Brief Description J. Chinese Journal of Geology, Jul, 3, (1990), 269-277.
- Gretener, P E: Geothermics: Using Temperature in Hydrocarbon Exploration[M], Beijing: Petroleum Industry Press, (1988), 31-33.
- Guo, T. T.: A Study on Thermal Sea and Field and Causes in Yunnan Tengchong Thermal Sea and Field. A doctoral thesis of Kunming University of Science and Technology, (2012), 67.
- Han, X. J. and Jin, X.: Analysis of Geothermal Resources and Thermal Structure in China's Northeastern Area J. Geology and Exploration, Jan, 38(1), (2002), 74-76.
- Hu, X. C.: Elementary introduction to the characteristics of deep heat source and heat-transfer in Yang Bajain Geothermal field[C]. Geological Publishing House: Proceedings of the International Symposium on high temperature geothermal exploitation and utilization in Tibet, China, Tibet Lhasa, (1992), 60-63(in Chinese with English abstract).
- Jiang, L., Ji, J. Q. and Xu, Q. Q.: Geological Analysis of Enhanced Geothermal System (EGS) in Baihai Bay Basin J. Geology and Exploration, Jan., 49(1), (2013), 167-178.
- Jiang, M., Tan, H. D. and Zhang, Y. W.: Physical Geography Model of Mazhan-Gudong Magma Pocket in Yunnan Tengchong Volcano Structure Area. Acta Geoscientia Sinica, Sept., 33(5), (2012), 731-739.
- Lee, W H K.: On the global variations of terrestrial heat flow J. Phys. Earth Planet. Inter, 2, (1970), 332-359.
- Li, K. W., Wang, L. and Mao, X. P.: Evaluation of Oil Gas Associated Geothermal Resources and Efficient Development J. Science & Technology Review, 2012.30 (32), (2012), 32-41.
- Liu, H. Y.: Analysis of Temperature and Pressure of Well ZK212 on Yangyi Geothermal Field in Tibet[D], China University of Geosciences (Beijing) Master Thesis, (2014), 24-25(in Chinese with English abstract).
- Lovering, T S.: Theory of heat conduction applied to geological problems[J]. GSA, 46(1), (1959), 69-93.
- Mundry, E.: Ueber die abkühlung magma tischer korper [J]. Geol Jahrb, 85(1), (1968), 755-766.
- Oskooi, B, Pedersen, L B and Smirnov M: The deep geothermal structure of the Mid-Atlantic Ridge deduced from MT data in SW Iceland, Phys. Earth Planet. Inter., 2005, 150(1-3), (2005), 183-195.
- Qiu, N. S.: Rock Heat Conductivity and Heat Generation Rate Characteristics in China's Northeastern Basins J. Geological Science, Apr., 37(2), (2002), 196-206.
- Rikitake, T.: Studies of the thermal state of the earth, Part 2 heat flow associated with magma intrusions [J]. Bull Earthq Inst, Tokyo, 37(2), (1959), 1584-1596.
- Shen, X. J. and Wang, Z. R.: Geothermal Reservoir Model Analysis for Tibet Yangbajing Geothermal Field. Science China B Volume, Oct. 1984, 10, (1984), 941-949.
- Tao, S. Z. and Liu, D. L.: Tanlu Fault Zone and Neighboring Geothermal Field Characteristics, Factors for Hot Spring Formation and Gas Composition J. Natural Gas Industry, 20(6), (2000), 42-47.
- Tester, J, Blackwell, D and Petty S: The future of geothermal energy: An assessment of the energy supply potential of engineered geothermal systems (EGS) for the United States [C]//Proceedings of Thirty-second Workshop on Geothermal Reservoir Engineering, Stanford, CA: Stanford University, January 22-24, (2007).
- Tian, W. G., Jiang, Z. X., Pang, X. Q., Meng, Q. Y. and Fu, L. X.: A Study on Magmatic Thermal Simulation and Its Source Rock Thermal Evolution Pattern J. Journal of Southwest Petroleum Institute, Feb., 27(1), (2005), 12-16.
- Urzua, L., Powell, T and Cumming W B: Apacheta, a New Geothermal Prospect in Northern Chile. Geothermal Resources Council Annual Meeting, (2002).
- Wang, J. Y., Hu, S. B., Pang, Z. H. and He, L. J.: Assessment of China Mainland Dry Heat Rock Geothermal Resources J. Science & Technology Review, 2012,30(32), (2012), 25-31.
- Wang, L. S., Liu, S. W., Xiao, W. Y. and Li, C.: Characteristics of Terrestrial Heat Flow Distribution in Bohai Sea Basin J. Chinese Science Bulletin, Jan. 2002, 47(2), (2002), 151-155.
- Wang, S. B., Fu, J. L., Li, C. Z., Jiang, F. C. and Tian, G. Q.: Initial Division of Active Stage of New Structure in Yunnan Southwestern Tengchong Plot. Geological Bulletin of China, Jan., 34(1), (2015), 146-154.
- Wu, Z. H., Hu, D. G., Liu, Q. S. and Ye, P. S.: Nyenchen Tanglha Granite Rock Thermal Evolution History and Thermochronology Analysis of the Ridge Uplifting Process J. Acta Geoscientia Sinica, Dec., 26(6), (2005), 505-512.
- Wu, Z. H., Jiang, W., Zhou, J. R. and Li, J. X.: Thermochronology Analysis of Qinghai-Tibet Plateau Interior Typical Rock Mass Thermal History and Structure-Landform Evolution Process. Acta Geologica Sinica, Nov. 74(4), (2001)468-476.

- Xiong, L. P. and Zhang, J. M.: Relation between North China Plain Geothermal Gradient and Base Structure Form. *J. Chinese Journal of Geophysics*, Mar., 31(2), (1988), 146-155.
- Yan, D. S. and Yu, Y. T.: Evaluation and Utilization of Geothermal Resources in Beijing, Tianjin and Hebei Oil Gas Area. *J. Wuhan: China University of Geosciences Press*, (2000).
- Yao, Z. J., Zhang, T. G., An, K. S., Zhen, Z. H.: Evaluation of Geothermal Resources in Tibet Yangbajing. *Chinese Academy of Geological Sciences Hydrogeology Engineering Geology Research Institute Journal*, No.2, 12, (1986).
- Zhang, Q., Jin, W. J., Li, C. D. and Jiao, S. T.: Cognition of "Magmatic Thermal Field" in Geothermal Field and Its Significance. *Progress in Geophysics*, Oct., 28(5), (2013), 2495-2507.
- Zhao, C. P., Ran, H. and Chen, K. H.: Today's Temperature in Magma Pocket within Crust of Tengchong Volcano Area: Estimation of Fractionation Effect of Carbon Isotope CO₂ and CH₄, Hot Spring Emergent Gas. *Acta Petrologica Sinica*, 27 (10), (2011), 2883-2897.
- Zhou, R. L., Liu, Q.S., Zhang, J. and Yang, L. Q.: North China Graben Basin Niutuozen Base Rock High Protruding Thermal Field Characteristics and Its Development Prospect. *Chinese Academy of Geological Sciences 562 Battalion Journal*, No. 7.8, (1989), 21-36.